Refereed Proceedings

The 13th International Conference on Fluidization - New Paradigm in Fluidization Engineering

Engineering Conferences International *Year* 2010

MAGNETIC RESONANCE (MR) MEASUREMENTS OF THE MASS FLUX IN GAS-SOLID FLUIDIZED BEDS

Andrew J. Sederman* Daniel J. Holland† L. F. Gladden‡
J. S. Dennis** C. R. Müller††

*University of Cambridge, ajs40@cam.ac.uk
†University of Cambridge, djh79@cam.ac.uk
‡University of Cambridge
**University of Cambridge
††ETH Zurich

MAGNETIC RESONANCE (MR) MEASUREMENTS OF THE MASS FLUX IN GAS-SOLID FLUIDIZED BEDS

C.R. Müller[2], D.J. Holland[1], A.J. Sederman[1], L.F. Gladden[1], J.S. Dennis[1]
[1]Department of Chemical Engineering and Biotechnology, University of Cambridge, Pembroke Street, Cambridge CB2 3RA, United Kingdom.
[2]Institute of Energy Technology, Department of Mechanical and Process Engineering, ETH Zurich, 8092 Zurich, Switzerland.

ABSTRACT

Magnetic Resonance (MR) Imaging was used to measure the time-averaged voidage and particle velocity in a 3D gas-solid fluidized bed. Two different distributors were used. The mass-flux through a horizontal plane was calculated by combining the local voidage and particle velocity measurements. Based on the conservation of mass it was possible to give an error in the combined voidage and particle velocity measurements. It was found that the error in the mass flux was usually small (< 5%), albeit increasing with increasing fluidization velocities.

INTRODUCTION

Single- and two-phase granular systems are commonly encountered in, for example, the pharmaceutical, energy-generation and agricultural industries. The ability to simulate two-phase granular systems numerically has improved significantly over the last two decades. However, the acquisition of detailed experimental measurements to validate these simulations is still extremely difficult, the major problem being that granular systems are visually opaque. Only a few experimental techniques exist to provide non-intrusive measurements in granular systems. Among these, the most important are Positron Emission Particle Tracking (1), Electrical Capacitance Tomography (ECT) (2), X-Ray attenuation (3) and Magnetic Resonance (MR) Imaging. The advantage of MR (4-7) is that it can measure the distribution of solids (voidage), and their velocities, in both single- and two-phase granular systems, whereas, *e.g.* ECT is limited to measurements of the void fraction and the velocity of voids, *i.e.* the rise velocity of bubbles and slugs. MR has previously been applied to study the motion and mixing of solids in a variety of granular systems, *e.g.* segregation in rotating cylinders (8), the dynamics of vibro-fluidized beds (9) and the behaviour of aspects of gas-solid fluidized beds (4-7, 10, 11). Additionally, measurements of the gas velocity and gas exchange between the bubble and emulsion phases in a fluidized bed have been published (12). A detailed literature review of the use of MR in process engineering can be found in (13).

The experimental quantification of the void fraction in gas-solid systems is further complicated by the difficulty of estimating the error in the measurement. In MR, the calibration of measurements of voidage is based on the theoretical result that there is a linear relationship between the signal intensity and voidage (14). To quantify the relationship, two measurements are usually made in a static system, in which voidage is known unequivocally for two cases, *viz.* a tapped bed and an empty bed.

In dynamic systems, such as two-phase flows, an estimate of the error in the voidage measurement can be calculated from a signal-to-noise analysis of the measurement (15). However, there are no available methods for experimentally testing the accuracy of these estimates directly.

One possibility for investigating the accuracy of measurements of voidage is to consider the conservation of mass flux. This has the added benefit of simultaneously providing a test of the accuracy of measurements of velocity. The principle here is that, in a two-phase granular system, *e.g*. a bubbling gas-fluidized bed, the time-averaged mass flux of particles crossing a horizontal plane has to be zero, assuming that no particles leave the bed. In this paper, we investigate this technique: MR measurements of the time-averaged voidage and velocities of particles in a 3D gas-fluidized bed were combined to calculate the flux of material crossing a horizontal plane. The deviation of the time-averaged flux from its zero value was used to give an absolute error in the combined measurements of the voidage and particle velocities.

EXPERIMENTAL

Apparatus

Measurements were made in a bubbling fluidized bed contained in an acrylic tube (i.d. 50 mm, o.d. 60 mm) placed vertically within the MR equipment. Two different distributors were used: (a) a porous glass frit, and (b) a perforated plate distributor containing 37 holes, each 1 mm in diameter. The pressure drop across these distributors was at least equal to that across the fluidized bed, at typical operating conditions (293 K, atmospheric pressure). The bed was fluidized by air supplied by a compressor and controlled using an Omega FMA 5443 mass flow controller. For the perforated plate distributor the gas was humidified prior to entering the fluidized bed to minimize electro-static effects; this was not possible for the porous frit distributor due to its high pressure drop.

The oil present in certain seeds is detectable by MR and serves as a means of detecting particles of interest. Poppy seeds (diameter, d_p = 1.2 mm, density, ρ_p = 950 kg/m^3, measured gas velocity at minimum fluidization at 293 K, U_{mf} = 0.3 m/s, Geldart's group B/D) were used as the fluidized particles. Poppy seeds contain a high fraction of mobile oil and thus have favourable T_1 and T_2 relaxation time constants (~400 ms and ~100 ms, respectively) for MR studies. The tapped bed height was H_o = 30 mm. The flowrate of air supplied to the apparatus was adjusted to allow superficial fluidizing velocities in the range, U = 0.375 – 0.63 m/s, equivalent to U/U_{mf} = 1.25 – 2.1.

MR imaging

Magnetic resonance experiments were performed using a Bruker DMX 200 spectrometer operating at a proton (^{1}H) frequency of 199.7 MHz. A birdcage radio frequency (r.f.) coil (i.d. 64 mm) was situated around the outside of the fluidized bed and was used to excite and detect the seeds. Spatial resolution was achieved using a 3-axis shielded gradient system capable of producing a maximum magnetic field gradient of 0.139 T m^{-1}.

The voidage was measured using a conventional spin-echo sequence to measure the distribution of the poppy seeds, *i.e*. solid fraction, in a horizontal (*x*-*y*) slice. The spin-echo images were acquired at a resolution of 32 × 32 pixels and with a sweep width of 76 kHz. The field-of-view was 55 mm × 55 mm in the *x*-*y* plane, yielding a spatial resolution of 1.72 mm × 1.72 mm. The echo time was kept as short as possible, *i.e.* 1.77 ms. The slice thickness was 5 mm. The centre of the slice was located 20 mm above the distributor. The spin-echo measurements were performed with TR = 1.5 s and 40 averages taken, resulting in a total acquisition time of ~ 1320 s.

The velocity of the particles was measured using a MR imaging sequence with two shaped gradient pulses to encode the velocity, each gradient pulse comprising the first half-period of a sine wave. The phase in an image obtained using this technique is proportional to the velocity of particles. The MR sequence is given in Fig. 1. The spin-echo images were acquired at a resolution of 64 × 32 pixels, resulting in a spatial resolution of 0.86 mm × 1.77 mm. The sine gradient was applied for δ = 591 μs with an amplitude of 0.0278 T m^{-1}. The time delay between the two velocity gradients was Δ = 2118 μs. The slice thickness was 5 mm and a sweep width of 76 kHz was used. To ensure that both the velocity and the voidage measurements had the same spatial resolution, the 64 × 32 acquisition array of the velocity measurements was truncated into a 32 × 32 array prior to applying the Fourier transform.

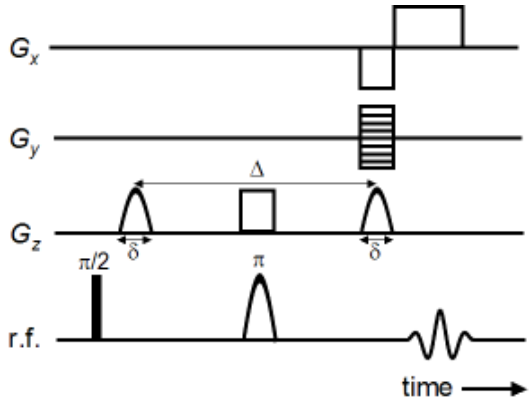

Figure 1 MR pulse sequence for the slice selective velocity measurements. A spin-echo sequence is used as the underlying imaging sequence. Velocity encoding is achieved by applying two lobes of a sine-shaped flow gradient on either sides of the soft π pulse.

Calibration

The calibration of the voidage measurements was performed by considering two stable states of the bed: a densely packed, tapped bed and an empty bed. For the poppy seeds, the tapped-bed voidage, $\varepsilon_{tapped,}$ was measured to be 0.32 ± 0.02 (15). Using quantitative MR images of the signal intensity, *I*, the spatially-resolved voidage of the fluidized bed, $\varepsilon(x,y)$, was calculated from:

$$\varepsilon(x,y) = 1 - \left(1 - \varepsilon_{\text{tapped}}\right)\frac{I(x,y)}{I_{\text{tapped}}(x,y)} \qquad (1)$$

where I_{tapped} is the signal intensity of the tapped bed. The flux of mass across a horizontal plane, m_z, was calculated from:

$$m_z = \sum_A (1-\varepsilon)\rho_p v_z dA \qquad (2)$$

where ρ_p, dA and v_z are, respectively, the density of the seeds, the area of a voxel and the velocity in the *z*-direction*, i.e.* normal to the horizontal (x-y)-plane considered.

Calculation of the error of the MR measurements

(i) Estimate of the error in the measurements of voidage

For the measurements of voidage, an estimate of the error in the measurement is given by a simple signal-to-noise ratio (SNR) analysis. This approach has been demonstrated by Holland *et al*. (15) and is summarized briefly as follows. First, the mean signal intensity, μ, outside the bed is calculated from the experimental measurements. Assuming a Rayleigh distribution of the magnitude of the MR signal (15), the standard deviation of signal intensity, σ, outside the bed is calculated from the mean signal intensity, μ, by:

$$\sigma = \sqrt{\frac{2}{\pi}} \cdot \mu \,. \qquad (3)$$

The standard deviation, σ, can be converted into a relative error in the measurement of voidage by dividing σ by the maximum signal intensity inside the bed (15).

(ii) Estimate of the error in the measurements of velocity

The error in the measurements of velocity can be estimated in a similar manner to the estimates of the error in the measurement of voidage. Again, the deviation of signal intensity outside the bed is calculated according to Eq. (3). An estimate of the error in the measurement of velocity is then given by dividing σ by the maximum signal intensity inside the bed and the phase shift in each voxel (16). Consequently, the error in the measurement of the velocity is inversely proportional to the phase shift and thus particle velocity. The phase shifts acquired in this study typically ranged between approximately –1 and 3.

(iii) Error in the mass flux measurements

Assuming that no particles leave the bed, conservation of mass dictates that the time-averaged mass flux across a horizontal slice has to be zero. Therefore, the absolute error of the mass flux measurements is given by the deviation of the time-averaged flux from its zero value.

To give an estimate of the relative error of the mass flux measurements, the deviation

of the time-averaged flux from its zero value is divided by the "absolute" mass flux, which we define as:

$$|m_z| = \sum_A (1-\varepsilon)\rho_p |v_z| dA \qquad (4)$$

RESULTS AND DISCUSSION

MR measurements of the voidage, ε, velocity, v_z and mass flux m_z are presented for both a porous frit and perforated plate distributor. This is followed by a discussion of the calculated error in the measurements of mass flux.

(i) Porous frit distributor

Figure 2 shows (a) the voidage, ε , (b) the velocity, v_z and (c) the mass flux m_z in a horizontal slice for U = 0.525 m/s (U/U_{mf} = 1.75). It is evident from Figs. 2(a-c) that the centre of the bed has both a high positive velocity and a high voidage, while there is a low voidage in the annular region near the wall. It is interesting to note in Fig. 2(b) that the highest negative velocity was measured in close proximity to the central upwards-flowing region, whereas the velocity and, consequently, also the mass flux are close to zero in the vicinity of the wall. This is consistent with a flow pattern induced by small bubbles rising through the centre of the bed. The observed flow-profile is consistent with measurements reported in (6,14).

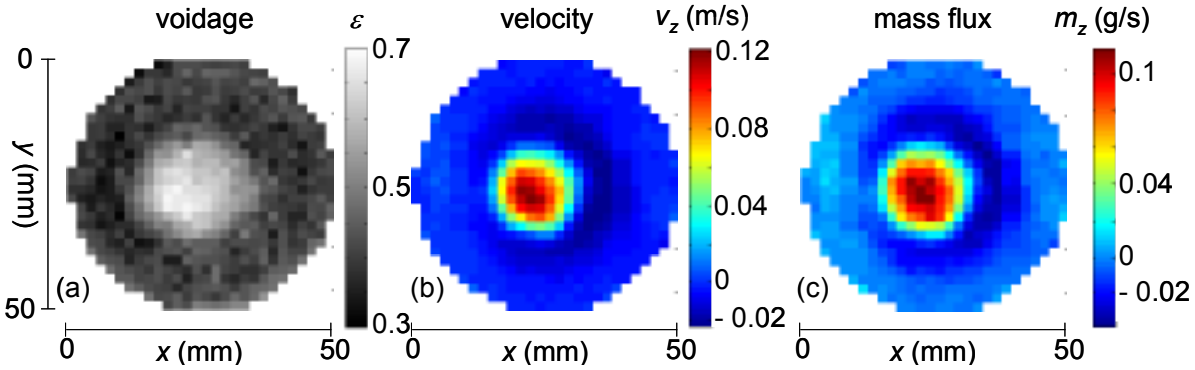

Figure 2 MR measurements of (a) the voidage, ε, (b) the velocity, v_z, and (c) the mass flux m_z in a horizonal (x,y) plane. The fluidization velocity was U = 0.525 m/s (U/U_{mf} = 1.75) and a porous glass frit served as distributor. The centre of the bed has both a high positive velocity and a high voidage.

(ii) Perforated plate distributor

MR measurements of (a) the voidage, ε , (b) the velocity, v_z and (c) the mass flux m_z in a horizontal slice for U = 0.525 m/s (U/U_{mf} = 1.75) using a perforated plate distributor are presented in Figs. 3(a-c), respectively. From Fig. 3(b) it can be seen that two regions of high positive velocity exist. These regions are also seen to have high voidage as can be observed in Fig. 3(a). This behaviour is quite distinctly different from the velocity profile observed at the same fluidization velocity for the porous frit distributor. In

Fig. 3(b) it can be seen that the regions of negative velocity extend to the walls of the bed, whereas, for the porous frit, the region of negative velocity was limited to an annulus close to the centre of the bed. The flow profile shown in Fig. 3(b) is consistent with measurements reported by Rees *et al.* (18).

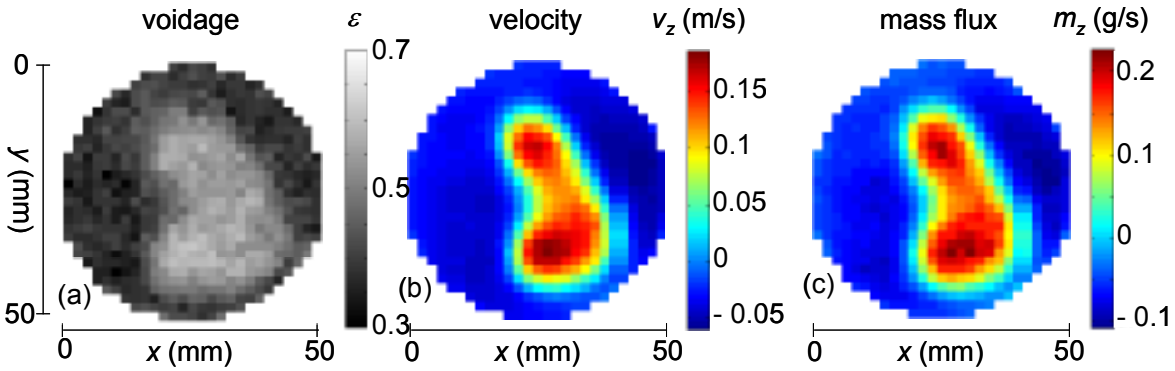

Figure 3 MR measurements of (a) the voidage, ε, (b) the velocity, v_z, and (c) the mass flux m_z in a horizonal (x,y) plane. The fluidization velocity was U = 0.525 m/s (U/U_{mf} = 1.75). A perforated plate containing 37 holes each of 1 mm diameter served as distributor. The region of high positive velocity and voidage in the perforated plate system is not axisymmetric but includes two local maxima.

The influence of the fluidization velocity on the flow profile for a perforated plate distributor is given in Figs. 4(a-c), showing the velocity v_z for U = 0.375 m/s (U/U_{mf} = 1.25), U = 0.525 m/s (U/U_{mf} = 1.75) and U = 0.63 m/s (U/U_{mf} = 2.1), respectively. At a superficial gas velocity of U = 0.375 m/s there are two regions with high positive velocity. With increasing fluidization velocity, these regions move closer together, merging into one region of high positive velocity at U = 0.63 m/s. It is also interesting to note from Fig. 4(a) that for the smallest fluidization velocity, the region close to the walls reveals time-averaged particle velocities close to zero. This is very similar to the behaviour observed for the porous frit distributor at U = 0.525 m/s. Considering the experimental measurements of Rees *et al*. (18), which show that the average jet height is ~ 10 mm for U/U_{mf} = 1.4, which is just below the position of the excited slice, it is not surprising that there is a distinct difference in the flow profiles using either a perforated or a porous frit distributor. However, a detailed analysis of the origin of the differences is beyond the scope of this paper. The flow profiles obtained using the perforated plate distributor provide a good contrast to the smooth, almost parabolic flow profiles obtained using the porous frit distributor. Thus, the different distributors enabled the measurement of the mass flux in both ideal and non-ideal flow conditions. Thus, it was possible to derive errors in the measurements of the mass flux, which are representative of mass flux measurements in a large variety of two-phase granular systems.

(iii) Error in the mass flux measurements

Based on the measurements shown in Figs. 3 and 4 it is possible to calculate the errors

in the mass flux and voidage measurements. The absolute mass fluxes and the calculated errors are summarized in Table 1. From Table 1, it can be seen that for most of the cases the error in the mass flux measurements is quite small, *i.e.* < 5 %. Errors of less than 5 % are also calculated for the voidage measurements. This is in agreement with voidage errors reported in (15). The only exception is U/U_{mf} = 2.1 using a perforated distributor with a calculated error in the mass flux of ~ 8.5 %. A possible explanation for this larger error could be that for this case 40 averages are not sufficient to obtain a stationary, time-averaged measurement of the voidage and particle velocities. Repeating the experiments for U/U_{mf} = 2.1 and increasing the number of averages to 160, resulted in a relative error in the mass flux of 5.5 %, indicating that increasing the averaging time helps to reduce the error. A more detailed study of the averaging effect will be reported elsewhere.

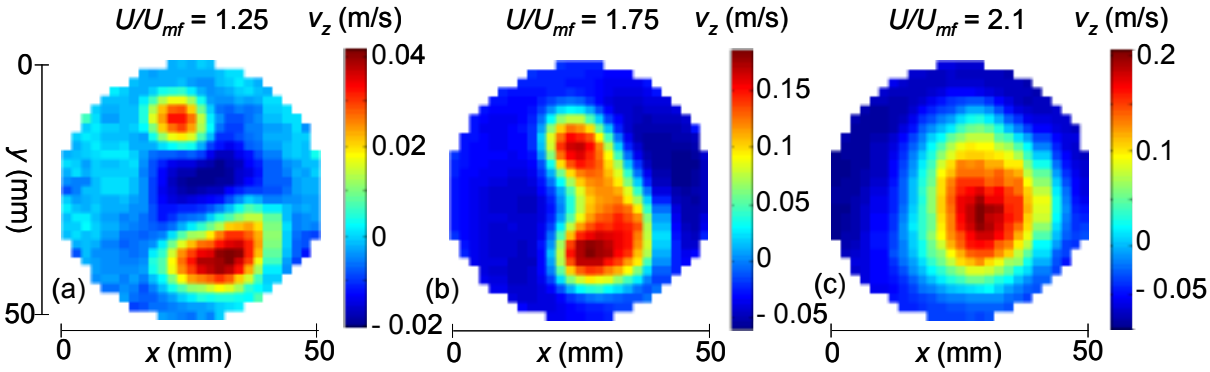

Figure 4 MR measurements of the velocity, v_z for different fluidization velocities: (a) U = 0.375 m/s (U/U_{mf} = 1.25), (b) U = 0.525 m/s (U/U_{mf} = 1.75) and (c) U = 0.63 m/s (U/U_{mf} = 2.1) using a perforated plate containing 37 holes each of 1 mm. At a superficial gas velocity of U = 0.375 m/s there are two regions with high positive velocity. With increasing fluidization velocity, these regions move closer together, merging into one region of high positive velocity at U = 0.63 m/s.

Table 1 The estimated error of the mass flux and voidage measurements. Estimates of the error are given for two different distributors and varying fluidization velocities.

Distributor	U - U_{mf} (m/s)	U/U_{mf}	Mass flux (g/s)	Error in mass flux (%)	Error in voidage (%)
Porous frit	0.252	1.75	0.2	+ 2.0	2.7
Perforated plate	0.075	1.25	0.3	+ 0.4	3.1
Perforated plate	0.252	1.75	1.9	- 4.0	3.2
Perforated plate	0.33	2.1	4.8	- 8.7	3.3

CONCLUSIONS

MR measurements of the voidage and particle velocities in a horizontal plane of a 3D gas-solid fluidized bed were obtained using two different distributors. Differences in the flow profiles using the different distributors were observed. Subsequently, the two MR techniques were combined to measure the mass flux in the fluidized bed. Assuming the conservation of mass, the time-averaged flux out of a horizontal plane in a bubbling fluidized bed has to be zero. It was shown that the calculated error was usually small, *i.e.* < 5 %, though seemed to increase with increasing values of U/U_{mf}.

ACKNOWLEDGEMENT

The authors would like to acknowledge the financial support of the EPSRC.

REFERENCES

1. M. Stein, Y.L. Ding, J.P.K. Seville, D.J. Parker (2000) Chem. Eng. Sci., **55**, 5291.
2. B. Du, W. Warsito, L.-S. Fan (2005) Ind. & Eng. Chem. Res., **44**, 5020.
3. P.N. Rowe, C.X.R. Yacono (1976) Chem. Eng. Sci., **31**, 1179.
4. C.R. Müller, J.F. Davidson, J.S. Dennis, P.S. Fennell, L.F. Gladden, A.N. Hayhurst, M.D. Mantle, A.C. Rees, A.J. Sederman (2006) Phys. Rev. Lett., **96**, 154504
5. C.R. Müller, D.J. Holland, J.F. Davidson, J.S. Dennis, L.F. Gladden, A.N. Hayhurst, M.D. Mantle, A.J. Sederman (2007) Phys. Rev. E, **75**, 020302.
6. D.J. Holland, C.R. Müller, J.S. Dennis, L.F. Gladden, A.J. Sederman (2008) Powder Technol., **182**, 171.
7. C.R. Müller, D.J. Holland, A.J. Sederman, M.D. Mantle, L.F. Gladden, J.F. Davidson (2008) Powder Technol., **183**, 53.
8. M. Nakagawa, S.A. Altobelli, A. Caprihan, E. Fukushima (1997) Chem. Eng. Sci., **52,** 4423.
9. C. Huan, X.Y. Yang, D. Candela, R.W. Mair, R.L. Walsworth (2004) Phys. Rev. E, **69**, 041302.
10. S. Harms, S. Stapf, B. Blumich (2006) J. Magn. Reson., **178**, 308.
11. R. Savelsberg, D.E. Demco, B. Blumich, S. Stapf (2002) Phys. Rev. E, **65**, 020301.
12. R. Wang, M.S. Rosen, D. Candela, R.W. Mair, R.L. Walsworth (2005) Mag. Res. Imag. **23**, 203
13. M.D. Mantle, A.J. Sederman (2003), Prog. Nuc. Magn. Reson. Spec., **43**, 3.
14. P.T. Callaghan, (1991) Principles of Nuclear Magnetic Resonance Microscopy.
15. D.J. Holland C.R. Müller, J.S. Dennis, L.F. Gladden, A.J. Sederman (2009) submitted to AIChE J.
16. E.M. Haacke, R.W. Brown, M.R. Thompson, R. Venkatesan (1999) Magnetic Resonance Imaging: Physical Principles and Sequence Design.
17. R.C. Darton, R.D. LaNauze, J.F. Davidson, D. Harrison (1977) Trans. Inst. Chem. Eng., **55**, 274.
18. A.C. Rees, J.F. Davidson, J.S. Dennis, P.S. Fennell, L.F. Gladden, A.N. Hayhurst, M.D. Mantle, C.R. Muller, A.J. Sederman (2006) Chem. Eng. Sci., **61**, 5702.